



QINJIANG SHANG obtained a BEng at the Architectural Engineering Department, University of Shiyou, in the Peoples' Republic of China in 1999. After working for some years in practice in China, performing reinforced concrete design, he enrolled for master's studies at the University of

Stellenbosch under supervision of Gideon van Zijl, with research topic shear behaviour of engineered cement-based composites. He was awarded the degree MScEng (Civil Engineering) by the University of Stellenbosch in December 2006.

Contact details:
T 021 808-4498
F 021 808-4947
@ gvanzijl@sun.ac.za



GIDEON VAN ZIJL is a part-time professor in Structural Engineering at the University of Stellenbosch (US), as well as a part-time research fellow at the Faculty of Architecture, Delft University of Technology (TUD), the Netherlands. He obtained a BEng and MEng (1990) at the US and a PhD

(2000) in Civil Engineering at the TUD. His research interests are construction materials, including design as well as physical and computational modelling of advanced cement-based materials. Concurrently, structural design guidelines and standards for existing and new cement-based construction materials are developed in his research group at the US.

Contact details:
T 021-808-4498
F 021-808-4947
gvanzijl@sun.ac.za

Characterising the shear behaviour of strain-hardening fibre-reinforced cement-based composites

Q Shang and G P A G van Zijl

Strain-hardening fibre-reinforced cement-based composites (SHCC) are a class of fibre-reinforced concrete (FRC) that, reinforced with relatively low volumes of short fibres, exhibit strain-hardening, tough tensile and flexural response. These qualities hold promise also for ductile, superior shear behaviour, which has been demonstrated in experimental projects internationally. The potential reduction or elimination of conventional steel shear reinforcement in reinforced concrete by the use of FRC, and in particular SHCC, is an example of how the tensile ductility properties of SHCC may be exploited. Other uses include generally improved ductility and durability of structures by selective use of these superior construction materials. However, the true shear behaviour of SHCC is not yet understood and analytical and design models have not yet been formulated due to a lack of an appropriate, accurate direct shear test method. This paper describes the investigation of the shear properties of SHCC. A modified Iosipescu shear test is developed for SHCC by finite element analysis. An experimental program of shear tests is subsequently reported, which aims to characterise the true shear mechanisms and properties of SHCC.

INTRODUCTION

Renewed interest in the structural use of fibre-reinforced concrete (FRC) has led to intensive research and development of these cement-based composites during the past decade. A particular class of FRC, namely strain-hardening fibre-reinforced cement-based composites (SHCC) has been developed for its superior tensile mechanical properties, yet containing relatively low quantities of short fibre to avoid the need for special mixing and placement techniques. As described in the paper (Boshoff & Van Zijl 2007) on page 24, the tensile ductility of SHCC approaches that of steel, while strain-hardening, or increased tensile resistance, follows crack initiation. As a result, SHCC is characterised by ultimate tensile strain and fracture energies of up to two orders of magnitude higher than conventional cement-based materials (Li & Wu 1992; Li & Leung 1992).

The shear failure of normal concrete reinforced with longitudinal steel occurs when principal tensile stresses within the shear span exceed the tensile strength of concrete and a diagonal crack propagates through the beam web. The brittle nature of concrete causes the collapse to occur suddenly after the formation of the first crack. With shear steel reinforcement, in the form of stirrups, the diagonal concrete cracks are controlled to some extent. However, although the overall shear resistance is

increased by stirrups, the eventual failure is brittle and dangerous, mainly because of large differences in deformability of steel and concrete. Several investigations towards the use of FRC and, to a lesser extent, SHCC (Fischer & Li 2002), to increase the post-peak toughness in shear failure have been performed. The excellent tensile ductility properties of SHCC give engineers a chance to overcome the brittle nature of normal concrete by partial or full replacement of concrete with SHCC in beams.

However, it is still a problem to describe accurately the true shear behaviour of SHCC due to a lack of an accurate test method. The determination of shear properties is regarded as one of the more difficult tasks in composite materials. The principal difficulty is the provision of a pure, uniform shear stress state in the specimen. Several shear test methods have been used in the past. A short, deep beam shear test is the most popular and simplest method, but it cannot provide a pure and uniform shear stress state in the specimen. Pure shear panel tests (Collins & Mitchell 1991) can create a pure shear stress state in the specimens, but the required facility is highly complicated and the shear stress in the specimen is not uniform. The Ohno shear beam test proposed in 1957 by K Ohno (in Japanese) creates a pure shear plane. This test has been applied in shear tests of a particular SHCC by Li *et al* (1994), which can be regarded as the first

Keywords: concrete, fibre-reinforced, shear, strain-hardening, Iosipescu

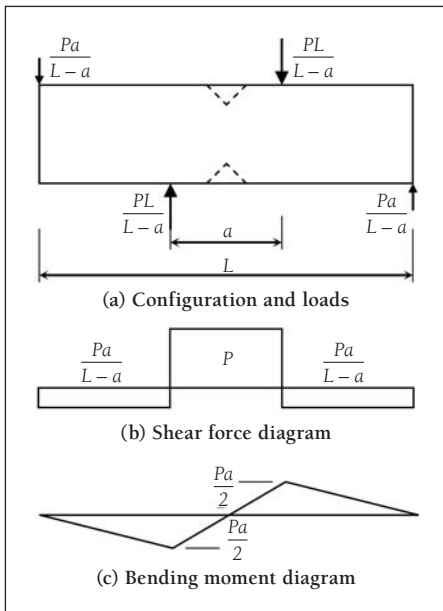


Figure 1 Shear test and internal forces shown schematically

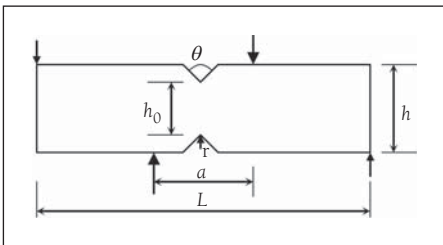


Figure 2 Basic configuration for Iosipescu shear test

attempt to evaluate the shear behaviour of these materials in more detail. However, the longitudinal reinforcement used in these tests to prevent flexural failure of the specimen most likely caused initiation of cracks near the beam top and bottom surface, which subsequently propagated diagonally into the pure shear zone (Kabele 2005), whereby objective distinction of the shear characteristics of SHCC becomes impossible. In an improvement on the Ohno test, a notched specimen was proposed by Iosipescu (1967), whereby a near uniform shear stress distribution in the pure shear plane became possible (Hodgkinson 2000). The method has since been studied and refined for shear testing of metals (Iosipescu 1967), fibre-reinforced plastics (Walrath & Adams 1985; Morton *et al* 1992), and wood (Xavier *et al* 2004). A standard test method for fibre-reinforced plastics has been adopted (ASTM 1993).

The Iosipescu test method is considered the best candidate test method for SHCC, but requires modifications for shear testing of these materials. This paper describes such modification by simple beam mechanics analysis and finite element (FE) refinement performed at the Institute for Structural Engineering (ISE), University of Stellenbosch. The specimen geometry is refined to cause a near uniform shear stress distribution in the plane of pure shear. In addition, it ensures that shear failure occurs

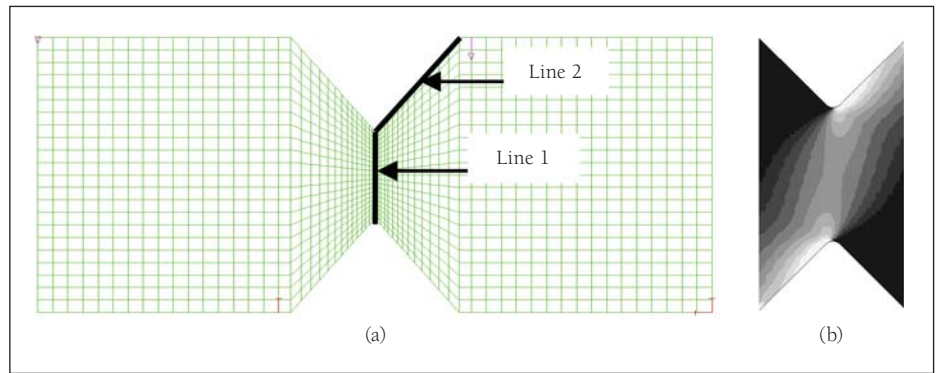


Figure 3 (a) FE model, with positions monitored for stress distributions; (b) contours of typical maximum principal stress field (white max, black min)

by avoiding higher principal stresses arising in regions outside this section. Thereby, not only elastic properties may be derived, but also strength and ductility. Subsequently, the shear response of a particular SHCC developed at the ISE is studied experimentally with this Iosipescu test to verify the test method and to improve the level of understanding of the shear behaviour of these materials.

IOSIPESCU SHEAR TEST MODIFICATION FOR SHCC

Simplified loading, shear, and moment diagrams are shown for the Iosipescu specimen in figure 1. Note that this is similar to the so-called Ohno shear test, the difference being a central notch in the Iosipescu specimen. It can be noted that in the centre of the specimen a constant shear force and a zero moment exist. The specimen geometry recommended in the ASTM Standard (ASTM 1993) is not suited for short, random fibre-reinforced cement-based materials. The ASTM specimens are small relative to the fibre length generally used in SHCC. Scaling-up of the size is required. Also, not only linear elastic properties are sought from this test for SHCC, but also strength and non-linear deformation response in shear. This requires an optimisation of the notch geometry with regard to the stress field in the notched area to ensure failure in the mid-plane while retaining a uniform shear stress distribution there. Therefore, a modified Iosipescu shear test specimen geometry for SHCC is developed here.

Geometrical proportioning by simple beam mechanics

Note that three types of failure modes can occur in the specimen, namely shear-dominated failure at the position of zero bending moment, bending-dominated failure at the position of maximum bending stress, and shear-flexure combined failure in the area in between. To establish a first geometrical shape and size, only the possibilities of shear failure at the notch and bending failure at the maximum bending moment are considered with simple analytical beam

theory, leading to the following requirement for shear failure in the notch:

$$h_0 < \frac{h^2}{3a \left(\frac{\tau_u}{\sigma_{tu}} \right)} \quad (1)$$

where h_0 is the notch height, h is the total height and a is the inner load spacing, as depicted in figure 2. In the derivation of equation 1 linear elasticity is assumed, with brittle failure in bending when the bending stress is reached, and brittle shear failure when the shear stress reaches a limit distributed uniformly over the notch middle plane.

To decide the global measurements of the shear specimens, comprehensive factors should be considered, which include the fibre length, as well as production, testing and cost of the specimen. A notch height of at least twice the fibre length was chosen to limit fibre alignment in cast specimens in the notch area. Based on this criterion a notch height of $h_0 \geq 24$ mm was chosen. An inner load spacing was chosen as $a = 80$ mm for practical execution of the experiment. By substituting a conservative, experiential

$$\text{ratio} \left(\frac{\tau_u}{\sigma_{tu}} \right) = 1,5 \text{ into equation 1 the}$$

minimum height of $h = 93$ mm is computed. However, a detailed FE sensitivity study to refine these values and other parameters, shown in figure 2, was envisaged. Therefore, the possibility of larger notch heights was anticipated, by choosing $h = 140$ mm.

As for the inner load point spacing, practical considerations governed the choice of overall length $L = 320$ mm. Finally, contact stress and potential compressive splitting failure in the load point regions were considered in the determination of the thickness, which was set to 20 mm. This thickness may be reduced to enforce two-dimensional, plane fibre orientation, while increasing the thickness will allow fully random three-dimensional fibre orientation in cast applications.

FE shear test refinement for SHCC

Next, FE sensitivity analysis was used to determine a suitable notch angle (θ) and

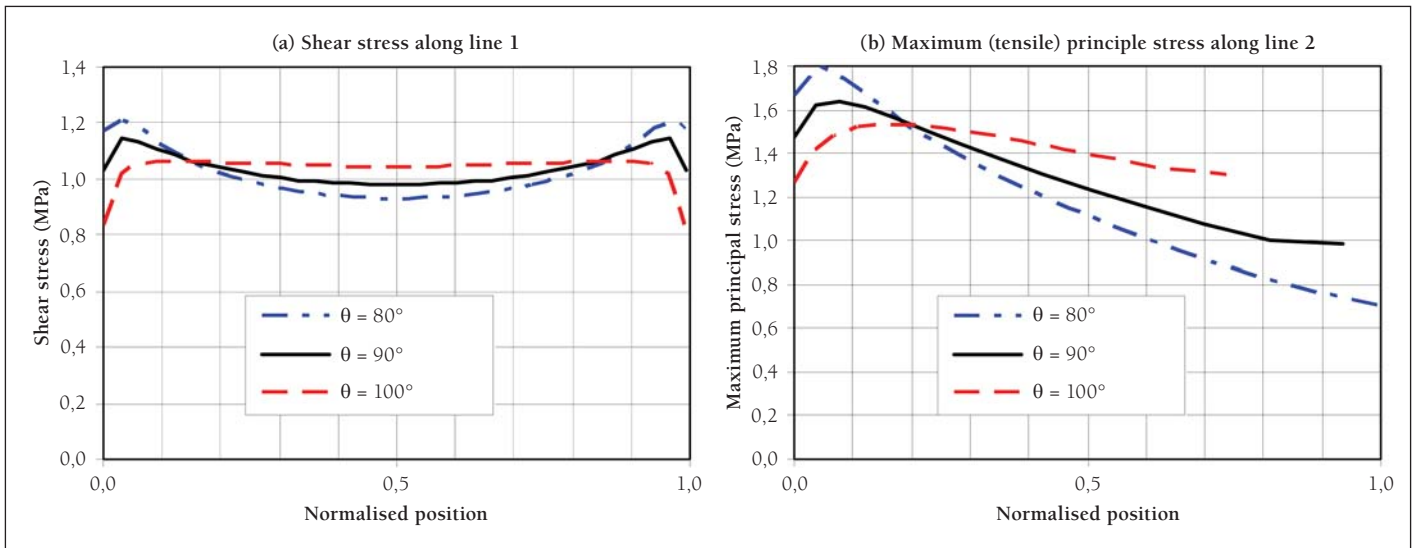


Figure 4 Normalised (a) shear and (b) tensile principal stress along line 1 (figure 3) and line 2 (figure 3) respectively

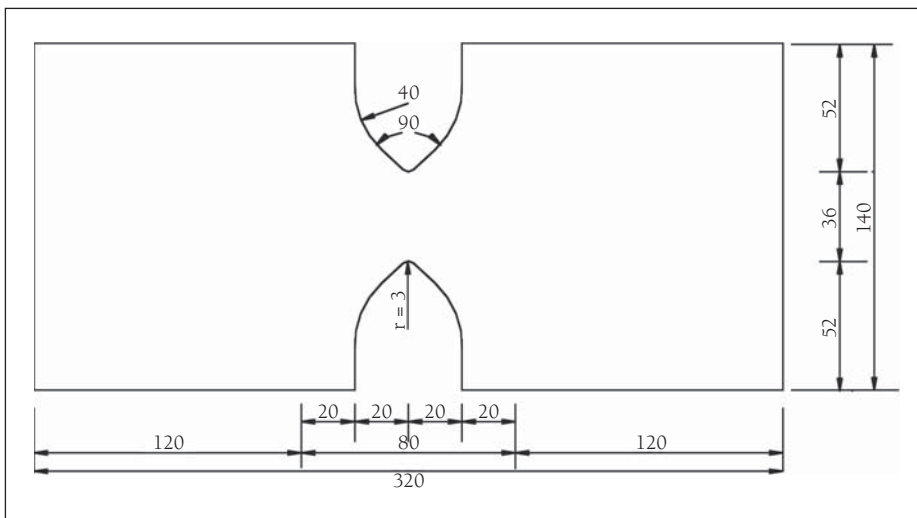


Figure 5 Refined SHCC Iosipescu shear specimen (all dimensions in mm)

notch tip radius (r), but also to study the notch height (h_0) influence on the stress field. The commercial FE software Diana (2002) was used. Simulations were carried out to determine the stress state in the elastic regime. Eight-node quadrilateral isoparametric plane stress elements and concentrated loads and supports were used in the analysis, as shown in figure 3a.

The purpose of refining the geometry of the specimen is to find a geometry which allows pure shear failure, that is, the failure of specimen occurs at the notch section, with a corresponding uniform shear stress along this notch section. Therefore, shear stress distributions along line 1 (figure 3a) are monitored. In addition, failure must initiate in the middle plane for objective shear stress characterisation. The location of the maximum principal stress is regarded as the position of failure initiation, because it is the well-known failure criterion for cement-based material. Based on the typical principal stress field (figure 3b), the maximum principal stress occurs along the upper (and lower) notch edges. Therefore, principal stress values were monitored along line 2 (figure 3a) to study the sensitivity of the potential failure

initiation position to variations in the mentioned geometrical parameters.

Therefore, the uniformity of shear stress along the line 1 and the location of the maximum principal stress in the line 2 are the two criteria for the geometrical refinement. Three different notch angles ($\theta = 80^\circ; 90^\circ; 100^\circ$), three different notch depth models ($h_0 = 24; 34; 44$ mm), and three different notch root radii ($r = 0; 2,7; 3,5$ mm) were implemented in the FE study. In figure 4 a selection of the FE results are shown, particularly for the shear stress variation along line 1 and the principal stresses along line 2 for the three different notch angles.

The most uniform shear stress distribution in the notch central plane is obtained for the largest notch angle ($\theta = 100^\circ$). The angle also reduces the maximum principal stress relative to the smaller notch angles, but shifts the position of peak principal stress farther away from the notch apex. Also, the principal stress gradient is smaller for the larger angle, whereby the principal stress in a larger part of the notch area away from the apex exceeds the principal stress in the apex, where failure is required. This means that crack initiation and propagation will occur farther away from

the pure shear plane for $\theta = 100^\circ$. For this reason the angle $\theta = 90^\circ$ is adopted for the SHCC shear test specimen.

A larger notch depth (h_0) increases the principal stress levels outside the pure shear plane due to increased bending stresses. However, within the range considered (24–44 mm), an insignificant influence on the ratio of the maximum peak principal stress along line 2 to the peak shear stress along line 1 was computed. The notch depth of 36 mm was adopted for practical handling of specimens and allowance for free fibre orientation.

Note that for a zero notch radius an infinite stress level exists theoretically in the notch apex. The introduction of a finite radius leads to a smooth stress transition whereby the stress peak at the apex is reduced to close to the average level. Insignificant improvement is brought about by further increase of the radius above 2,7 mm. The final geometry is shown in figure 5.

SHEAR TEST RESULTS

An experimental program was executed to test the SHCC Iosipescu test and specimen geometry designed in the previous section.

Materials design and processing

A SHCC material developed at the ISE (Gao & Van Zijl 2004) was used as basis for these shear tests. A standard matrix mix, but containing different fibre volumes, was used in the test program. The mix proportions are given in table 1. Polyvinyl alcohol fibre (PVA) was provided by Kuraray Co Ltd, Japan. Local Western Cape dune sand (Philippi) was sieved and graded to American standard F95 particle size distribution, which has a maximum particle size smaller than 0,3 mm.

The ECC was mixed in a Hobart three-speed laboratory mixer with 8 l capacity. For each batch of material, three Iosipescu shear specimens and three direct tension

Table 1 Ingredients and mass (in kg) of SHCC specimens

Type	Cement (CEM I 42.5)	Fly ash	GGCS (Saldanha)	Water	Sand (F95)	PVA V_f (%)	Number of specimens		
							Phase 1	Phase 2	Phase 3
S1	0,5	0,45	0,05	0,4	0,5	0,0	3		
S2	0,5	0,45	0,05	0,4	0,5	1,0	3		
S3	0,5	0,45	0,05	0,4	0,5	2,0	3	3	3
S4	0,5	0,45	0,05	0,4	0,5	2,5	3	3	3

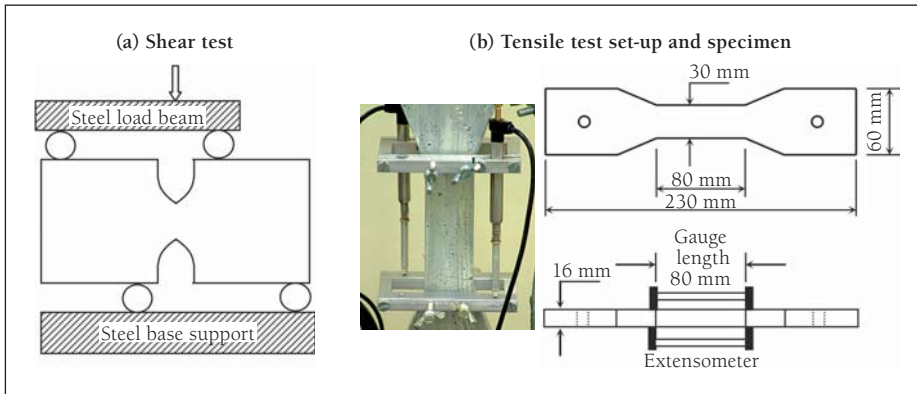


Figure 6 Test set-up

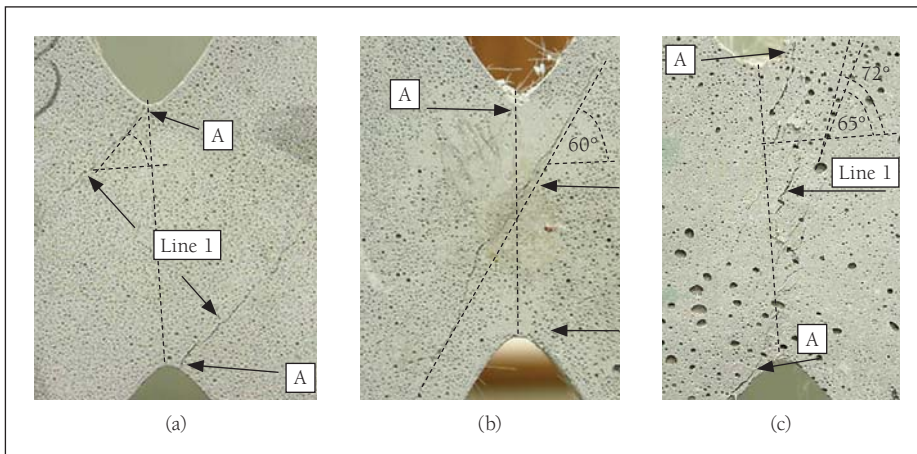


Figure 7 Typical failure crack patterns in (a) S1, (b) S2 and (c) S3 and S4 specimens

(dog-bone) specimens were cast. The shear and tension specimens were cast in specially designed perspex and steel moulds respectively. All specimens were moist-cured for three days before demoulding, and subsequently wet cured up to the age of 14 days in water of constant temperature (23 °C). All specimens were then tested wet at the age of 14 days.

Test set-up

Both the tensile tests and the shear tests were performed in a materials testing machine (Zwick Z250) operating under displacement control. A 5 kN load cell was installed to monitor the transmitted load with high accuracy in the low-force range applied. The shear tests were performed at a fixed displacement rate of 1,5 mm/minute of the crosshead, while the testing speed was 0,5 mm/minute for the direct tensile tests. A Spiderman8 data collector connected to a computer monitored the force results in both tests. This apparatus also collected strain

gauge and LVDT displacement measurements in the shear tests and LVDT displacement measurements in the direct tensile tests. The shear test set-up is shown in figure 6a and the direct tensile test in figure 6b.

To improve this new shear test method gradually, the tests are carried out in three phases. The aim of the first phase is to check if the failure of the specimen is a pure shear failure. The second phase is to obtain the shear stress and shear strain of the specimens with the pure shear failure mode, measured by the load cell and a strain gauge (type KFG-10-120-d17-11). In the third phase, information about the non-linear deformational response is obtained from diagonal LVDT (type HBM WA/10) measurement in the notch area.

Test results and discussion

Phase one: Shear failure mode

The typical shear failure mode for the specimens S1–S4 can be seen in figure 7. The

positions of crack initiation are similar in the four types of specimens, within 1–1,5 mm from the upper and lower notch tip. However, after crack initiation, the crack propagation and patterns differ significantly, depending on fibre content.

In the S1 specimens, with no fibre, two cracks propagate skew-symmetrically away from the notch area, with no other visible cracking. The specimens almost instantly fail following the first crack initiation. In the S2 specimens, with low fibre content ($V_f = 1\%$), the initial cracks are arrested and a new crack arises and propagates diagonally through the notch area at approximately 60°. This is the final crack pattern at failure. The modes of failure in S3 ($V_f = 2\%$) and S4 ($V_f = 2,5\%$) are similar, but are significantly different to that of S1 and S2. After first cracks occur, several microcracks appear in the notch area. The cracks develop to a length of about 5 mm. Finally, the microcracks are connected with vertical cracks, forming a final fracture surface close to the notch middle line.

The failure modes of the S1 and S2 are dominated by combined shear-flexure, with cracks extending well into the flexure zones. Therefore, for these specimens, this test method is not appropriate for the characterisation of the inelastic shear behaviour, including shear strength. In the S3 and S4 specimens, cracking is restricted to the central notch region, that is, close to the pure shear region. It can be argued that extra energy dissipation occurs in the diagonal cracks, where fracture surfaces arise in addition to the final failure fracture surface. However, this is the nature of SHCC, and this test method manages to capture this multiple cracking behaviour. Crack saturation occurs in the notch zone, whereby realistic representation of the macroscopic non-linear shear response is achieved in this test.

In the second phase, which is discussed next, the pseudo strain-hardening nature of the S3 and S4 specimens are confirmed by direct tensile tests. In earlier work the critical fibre volume to ensure strain hardening with this cement-based matrix was estimated to be $1\% < V_f < 2\%$ (Van Zijl & Boshoff 2006).

Phase two: Shear strain measurement

In this phase, direct tensile tests and Iosipescu shear tests were performed on specimens of type S3 and S4. First, three specimens each of S3 and S4 were tested in

Table 2 Iosipescu shear results for S3 and S4 specimens

		First crack shear stress τ_t (N/mm ²)	Ultimate crack shear stress τ_u (N/mm ²)	G-modulus (kN/mm ²)
S3	Specimen 1	3,64	3,98	3,01
	Specimen 2	3,38	3,97	2,55
	Specimen 3	3,55	4,02	2,84
	Average	3,52	3,99	2,80
StDev		0,13	0,03	0,23
COV		4 %	1 %	8 %
S4	Specimen 1	3,69	4,05	3,26
	Specimen 2	3,68	4,15	3,31
	Specimen 3	3,72	4,01	2,85
	Average	3,70	4,07	3,16
StDev		0,02	0,07	0,22
COV		1 %	2 %	7 %

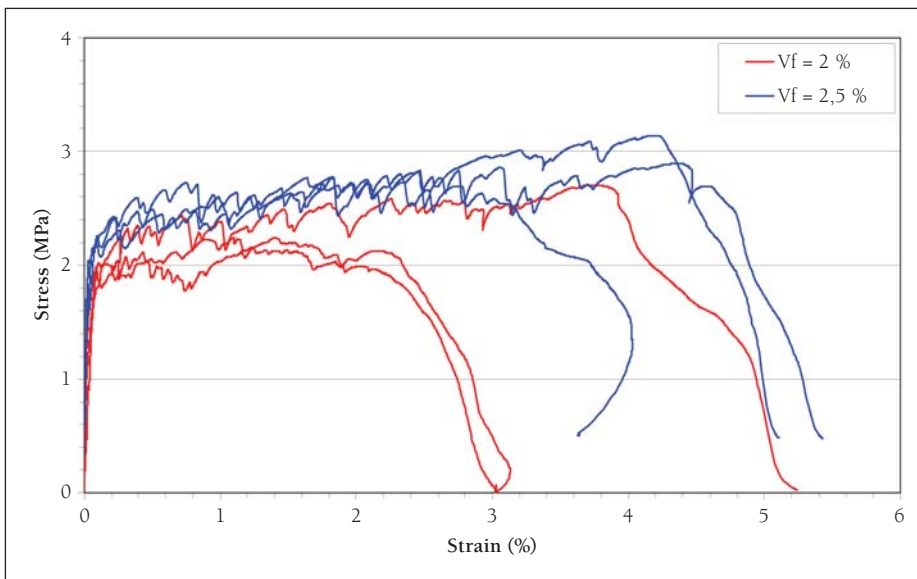


Figure 8 Uniaxial tensile stress-strain responses for S3 and S4 specimens

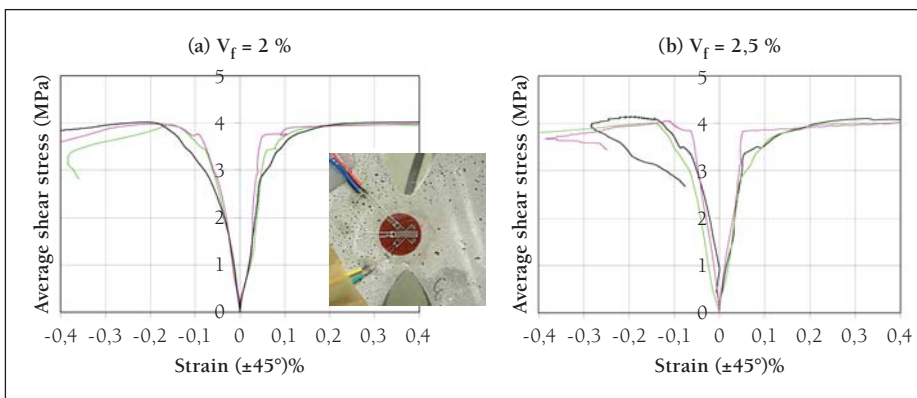


Figure 9 Shear stress vs principal strain responses for (a) S3 and (b) S4 specimens

direct tension to confirm that these specimens indeed exhibit strain hardening. The tensile stress-strain results are shown in figure 8, confirming that these specimens may be classified as SHCC.

In this phase the shear tests on S3 and S4 specimens were repeated, but with three new specimens of each type. Each specimen was instrumented with a single strain gauge rosette, to measure the relationship between the shear stress and strain. The strain gauges

were glued onto the surface of each specimen along the middle line at mid-height, as shown in the insert in figure 9. Results from these tests are shown in figure 9 in terms of the average shear stress in the notch middle plane and the diagonal tensile (+45°) and compressive (-45°) strain gauge measurements. It can be observed that the development of compressive and tensile strain in the two group specimens are similar in the elastic range, but differ in the inelastic range.

This is due to microcracks arising perpendicular to the tensile direction, significantly increasing the tensile deformation compared with the compressive deformation.

In the pure shear state the normal strains at $\pm 45^\circ$ are the principal strains. From standard strain transformation it can be shown that the shear strain is obtained by subtracting the compressive strain from the tensile strain. In figure 10 these engineering shear strains are plotted against the average shear stresses in the notch middle plane.

Further shear and tensile test results from this phase are tabulated in tables 2 and 3. Note that the elastic moduli (E) have been computed from uniaxial tensile stresses at one third of the first cracking stress and a pre-stress of $\sigma_0 = 0,1$ N/mm² and the corresponding strains as follows:

$$E = \frac{\frac{1}{3}\sigma_t - \sigma_0}{\epsilon_{(\frac{1}{3}\sigma_t)} - \epsilon_0} \quad (2)$$

The same procedure was followed to determine the shear modulus (G) from the Iosipescu shear test results as follows:

$$G = \frac{\frac{1}{3}\tau_t - \tau_0}{\gamma_{(\frac{1}{3}\tau_t)} - \gamma_0} \quad (3)$$

where $\tau_0 = 0,1$ N/mm² is a small pre-stress with corresponding shear strain γ_0 .

From the experimental results shown in tables 2 and 3 it can be seen that the variation in the shear strength (coefficient of variation (COV) $\leq 2\%$) and shear modulus (COV $\leq 8\%$) is reasonably low and acceptable. The variation in tensile strength properties is larger for both ultimate strength (COV $\leq 7\%$) and elastic modulus (COV $\leq 16\%$). Furthermore, the ultimate shear stresses are higher than the ultimate tensile stresses in both specimens by up to 49% in terms of average shear and tensile strength. With increasing fibre content, the ultimate shear stress and shear strain both increase.

Phase three: Inelastic shear strain measurement

Note that strain gauges are not capable of accurately capturing deformations that include cracks. This means that the non-linear strains shown in figures 9 and 10 beyond the initial approximately linear stress-strain response do not represent the true non-linear deformation in the Iosipescu specimens. Therefore, in the third phase of this experimental program, three more specimens of types S3 and S4 each were prepared and instrumented for LVDT displacement measurements in the maximum (tensile) principal strain direction (45°) as shown in the insert in figure 11. The measurements were taken over a gauge length of approximately

Table 3 Direct tensile results for S3 and S4 specimens

		First crack stress σ_t (N/mm ²)	Ultimate tensile stress σ_{tu} (N/mm ²)	Tensile strain capacity ϵ_F (%)	E-modulus (kN/mm ²)
S3	Specimen 1	1,94	2,53	2,52	8,5
	Specimen 2	1,84	2,64	2,70	6,5
	Specimen 3	1,52	4,76	2,82	7,2
	Average	1,77	2,68	3,31	7,4
StDev		0,22	0,15	1,26	1,0
COV		13 %	6 %	38 %	14 %
S4	Specimen 1	1,96	4,89	2,89	9,0
	Specimen 2	1,87	4,82	3,14	9,6
	Specimen 3	1,72	3,95	2,73	7,0
	Average	1,85	2,92	4,55	8,5
StDev		0,17	0,21	0,52	1,3
COV		9 %	7 %	11 %	16 %

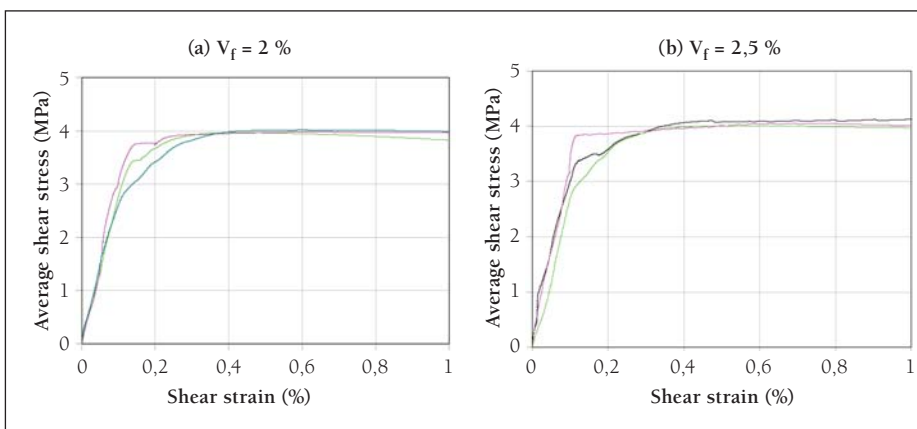


Figure 10 Shear stress vs shear strain responses for (a) S3 and (b) S4 specimens

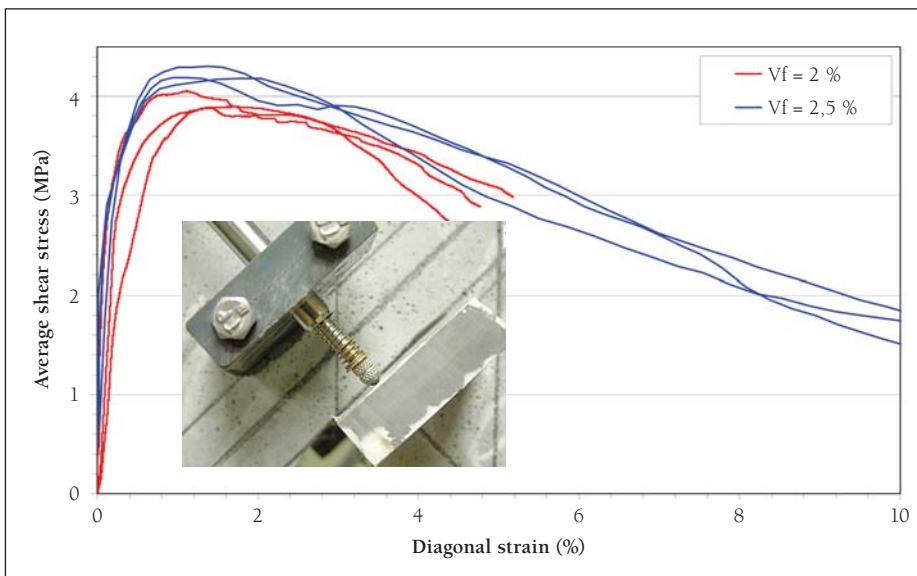


Figure 11 Shear stress vs diagonal strain measured by LVDT S3 and S4 specimens

25 mm. This gauge area extends into the flexural zones, so not only pure shear deformation is captured. Nevertheless, an indication of shear toughness is obtained, as can be seen in figure 11. These results also serve as verification of a computational model for SHCC, described in the paper on page 24 (Boshoff & Van Zijl 2007).

The shear strengths of these specimens are in agreement with the tabulated values of phase 2 (table 2), confirming the trend of increased strength with fibre content increase. It is apparent that the diagonal tensile responses shown in figure 11 are not strain-hardening, but rather strain-softening, forming an envelope for the direct ten-

sile responses shown in figure 8. However, the strain response at 45° in Iosipescu shear specimen does not represent a uniaxial tensile stress state as in the case of the direct tensile test specimens. In the shear specimens a biaxial (compressive-tensile) stress state occurs diagonally. Also, principal stress and strain rotation from the original ±45° orientation occurs in the non-linear regime, as will be discussed in the next section, towards understanding the shear behaviour of SHCC.

TOWARDS UNDERSTANDING SHCC SHEAR RESPONSE

By understanding the mechanisms governing shear response in cement-based composites it becomes possible to derive rational guidelines for analysis and design. However, such understanding is also required to ensure that objective characterisation is enabled by a particular test. In this section the observed shear responses are reflected upon with respect to the ability of the SHCC Iosipescu test to capture SHCC shear behaviour. In the paper (Boshoff & Van Zijl 2007) on page 24 the test is analysed with the aid of a constitutive model for SHCC developed and implemented in the FE package DIANA at the ISE.

The main mechanism of non-linear shear response of SHCC is diagonal exceedance of tensile elastic limit stress and subsequent formation of multiple cracks, as seen in figure 7c. In the reported Iosipescu test, the final shear failure mechanism is the interconnection of the multiple cracks and subsequent vertical shear-slipping along this crack plane. It must be noted that this failure pattern is not possible in brittle or softening materials, as was clearly shown in the failure patterns of the S1 and S2 specimens, with zero or low fibre content.

In the SHCC, of which the S3 and S4 specimens are examples, cracks are bridged by fibres, allowing the external force to be increased due to the reserve capacity in tension and, of course, compression. This is shown schematically in figure 12. When the tensile ‘yield’ strength is reached ($\sigma_1 = \sigma_2$), this can be maintained upon further increased load. However, for equilibrium with the increasing shear force (S), principal stress rotation is required to exploit the capacity in compression. Nevertheless, axial equilibrium must be maintained. These horizontal and vertical force equilibrium requirements can be expressed respectively as:

$$-\sigma_2 ht \cos^2(\theta) + \sigma_1 ht \sin^2(\theta) = 0 \quad (4)$$

$$\tau ht - \sigma_2 ht \cos(\theta) \sin(\theta) + \sigma_1 ht \sin(\theta) \cos(\theta) = 0 \quad (5)$$

Equation 4 can be rewritten in terms of the principal stress orientation as follows:

Table 4 Observed crack orientation and measured strength ratios for SHCC

V_f	θ	τ_u (MPa)	σ_t (MPa)	σ_{tu} (MPa)	τ_u / σ_t	τ_u / σ_{tu}
2	60–65°	3,99	1,77	2,68	2,25	1,49
2,5	60–65°	4,07	1,85	2,92	2,20	1,39

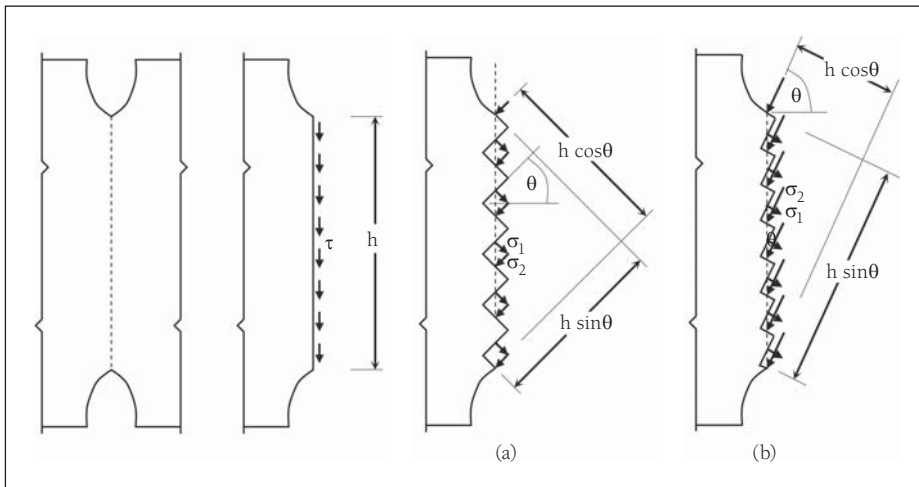


Figure 12 Schematic representation of principal stresses in failure plane in (a) elastic stage and (b) at failure

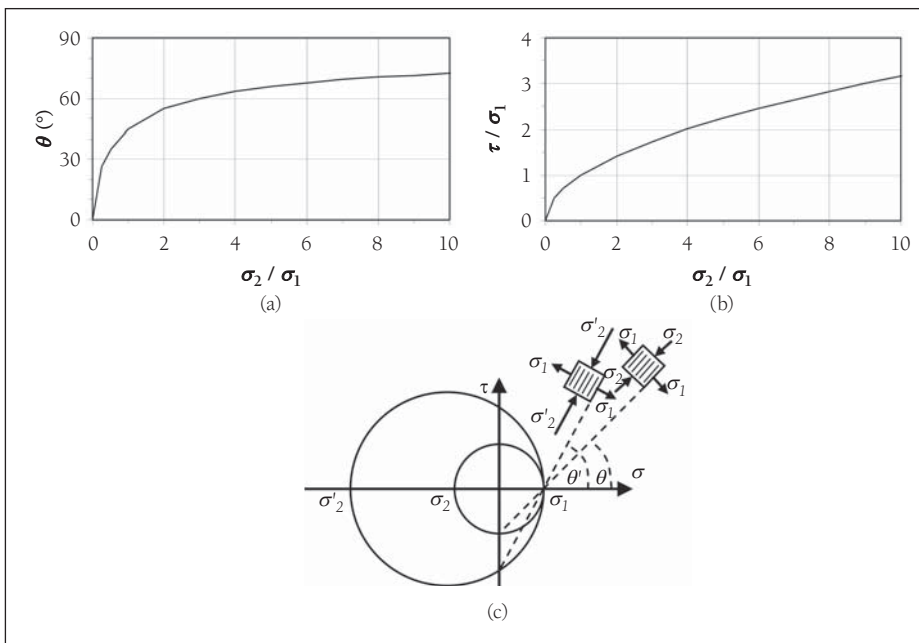


Figure 13 Prediction of (a) diagonal shear crack orientation and (b) shear strength to tensile strength for SHCC; (c) Mohr Circle illustration of principal stress rotation, crack alignment and shear stress increase

$$\theta = \tan^{-1} \sqrt{\frac{\sigma_2}{\sigma_1}} \quad (6)$$

And from equation 5 the average shear stress can be expressed as

$$\tau = \sigma_1 \left(1 + \frac{\sigma_2}{\sigma_1} \right) \sin \theta \cos \theta \quad (7)$$

If the typical ratio of compressive to tensile strength of 5–10 is substituted into equations 6 and 7, an angle of $\theta = 65,9^\circ - 72,5^\circ$ and a shear strength / tensile strength ratio of 2,2–3,2 are computed. See also figure 13(a) and (b) for a graphical representation of equations 6 and 7, and figure 13c for a Mohr Circle demonstration of the crack rotation and shear stress increase with

increased principal stress ratio. Of course, failure may occur before maximum compressive resistance is reached, so the lower ratio of principal stresses may be mobilised. Also, biaxial effects, that is, compressive resistance reduction upon orthogonal tension (or vice versa) will further alter the ratio. Nevertheless, these values are in reasonable agreement with the crack orientation seen in figure 7c and the ratio between average shear and tensile strength from tables 2 and 3, summarised in table 4.

Note that the condition for crack rotation is ductility, because failure is imminent in brittle materials when $\sigma_2/\sigma_1=1$ and when the tensile strength is reached ($\sigma_1 = \sigma_t$), because the compressive capacity cannot be mobilised. This explains the approximate

45° orientation of the cracks in the S1 and S2 specimens with subcritical fibre content.

The above reasoning explains the observed failure patterns and strengths. The question remains whether this test measures the true shear resistance, or whether the restriction of the failure to the notch apex enforces a higher mode of failure. This would imply that, by mobilising the multiple crack formation in the pure shear zone, the true shear response in the pre-peak shear load deformation is obtained in the test, but by enforcing these diagonal cracks to be linked vertically in the final failure plane, a shear compressive failure mechanism is mobilised, instead of shear crack propagation along the inclined cracks. Here, it is postulated that the latter is a combined tension-shear failure, as is most often found in reinforced concrete beams subjected to shear-dominated failure. This may indeed be a lower mode of failure for which the accurate prediction of SHCC resistance in such shear-slipping along an existing, propagating diagonal crack remains to be characterised. This will be studied in continued research by computational and experimental studying of the behaviour of deep beams without notches, where combined shear-flexural failure occurs.

DISCUSSION AND CONCLUSIONS

A modified Iosipescu test method has been developed for testing the shear behaviour of a new class of building material, namely strain-hardening fibre-reinforced cement-based composites (SHCC). Whilst the test enables objectivity in determining the elastic shear properties due to the pure, uniform shear stress field generated in the specimen, information of the non-linear behaviour is also obtained. By refinement of the specimen geometry, failure in the notch apex region of the specimen is enforced, whereby shear strength and ductility characterisation can be extracted from the test results.

The shear test has been verified in an experimental program, from which the following conclusions can be drawn:

- For SHCC failure occurs in the notch area in close vicinity of the apex region. Hereby the calculation of shear strength from the peak internal shear force and the notch section area is justified
- Multiple cracks arise, whereby the true nature of SHCC, as also exhibited in uniaxial tension, is mobilised
- The cracks develop at an angle dominated by the principal stress direction, which in turn depends on the compressive:tensile strength ratio. This can only be realised if sufficient ductility in tension allows the tensile resistance to be maintained at deformations beyond the first cracking deformation, to enable the compressive resistance to be mobilised

Future research will study the general applicability of this shear behaviour, specifically in combined flexure-shear, where a lower strength shear-slipping failure mechanism may dominate.

ACKNOWLEDGEMENT

The support of the Ministry of Trade and Industry through the Technology and Human Resources for Industry Programme (THRIP), as well as the industrial partners of the THRIP project 2660, APERC Structures, is gratefully acknowledged.

REFERENCES

ASTM D 5379 1993. Test method for shear properties of composite materials by the V-notched beam method. Philadelphia: ASTM.

Boshoff, W P and Van Zijl, G P A G 2007. A computational model for strain-hardening fibre-reinforced cement-based composites. *Journal of the South African Institution of Civil Engineering*, 49(2):24–31.

Collins, M P and Mitchell, D 1991. *Prestressed concrete structures*. Canadian Prestressed Concrete Institute.

Diana 2002. *Diana Finite Element Analysis User's Manual*, release 8.1. TNO Building, The Netherlands.

Fischer, G and Li, V C 2002. Influence of matrix ductility on tension stiffening behavior of steel reinforced Engineered Cementitious Composites (ECC). *ACI Structural Journal*, 99(1):104–111.

Gao, S and Van Zijl, G P A G 2004. Tailoring ECC for commercial application. Department of Civil Engineering, University of Stellenbosch, South Africa., *Proceedings of BEFIB Como, Italy*, pp 1391–1400.

Hodgkinson, J M 2000. *Mechanical testing of advanced fibre composites*. Cambridge: Woodhead Publishing.

Iosipescu, N 1967. New accurate method for single shear testing of metals. *Journal of Materials*, 2(3):537–566.

Kabele, P 2005. Fracture behaviour of shear-critical reinforced HPRCC members. *Proceedings of the workshop on HPRCC in structural applications*, Honolulu, Hawaii, USA, May 2005.

Li, V C and Wu, H C 1992. Conditions for pseudo strain-hardening in fiber reinforced brittle matrix composites. *Journal of Applied Mechanics Reviews*, 45(8):390–398.

Li, V C and Leung, C K Y 1992. Steady state and multiple cracking of short random fiber composites. *ASCE J. Eng. Mech.*, 118(11):2246–2264.

Li, V C, Mishra, D K, Naaman, A E, Wigh, J K, LaFave, J M, Wu, H C and Inada, Y 1994. On the shear behavior of engineered cementitious composites. *Journal of Advanced Cement Based Materials*, 1(3):142–149.

Morton, J, Ho, H, Tsai, M and Farley, G L 1992. A materials shear property measurement. *Journal of Composite Materials*, 26:708–750.

Van Zijl, G P A G and Boshoff, W P 2006. Verification of design formulae for the structural use of strain-hardening fibre-reinforced cement-based composites. In preparation.

Walrath, D E and Adams, D F 1985. Iosipescu shear properties of graphite fabric/epoxy composite laminates. University of Wyoming, Department Report UWME-DR-501-103-1.

Xavier, J C, Garrido, N M, Oliviera, M, Morais, J L, Camanho, P P and Pierron, F 2004. A comparison between Iosipescu and off-axis shear test methods for the characterisation of Pinus Pinaster Ait. *Composites Part A*, 35(7-8):827–840.